Journal of Environmental Management 145 (2014) 106–112

Contents lists available at ScienceDirect

Journal of Environmental Management

journal homepage: www.elsevier.com/locate/jenvman

Fundamental aspects related to batch and fixed-bed sulfate sorption by the macroporous type 1 strong base ion exchange resin Purolite A500

Damaris Guimarães, Versiane A. Leão*

Bio & Hydrometallurgy Laboratory, Department of Metallurgical and Materials Engineering, Universidade Federal de Ouro Preto, Campus Morro do Cruzeiro, s.n., Bauxita, Ouro Preto, MG 35400-000, Brazil

ARTICLE INFO

Article history:
Received 23 February 2014
Received in revised form
6 May 2014
Accepted 7 June 2014
Available online 9 July 2014

Keywords:
Sulfate
Mine water
Ion exchange resins
Fixed-bed models
Film diffusion
Surface diffusion

ABSTRACT

Acid mine drainage is a natural process occurring when sulfide minerals such as pyrite are exposed to water and oxygen. The bacterially catalyzed oxidation of pyrite is particularly common in coal mining operations and usually results in a low-pH water polluted with toxic metals and sulfate. Although high sulfate concentrations can be reduced by gypsum precipitation, removing lower concentrations (below 1200 mg/L) remains a challenge. Therefore, this work sought to investigate the application of ion exchange resins for sulfate sorption. The macroporous type 1 strong base IX resin Purolite A500 was selected for bath and fixed-bed sorption experiments using synthetic sulfate solutions. Equilibrium experiments showed that sulfate loading on the resin can be described by the Langmuir isotherm with a maximum uptake of 59 mg mL-resin^{-1}. The enthalpy of sorption was determined as +2.83 kJ mol^{-1}, implying an endothermic physisorption process that occurred with decreasing entropy (−15.5 J mol^{-1}.K^{-1}). Fixed-bed experiments were performed at different bed depths, flow rates, and initial sulfate concentrations. The Miura and Hashimoto model predicted a maximum bed loading of 25 −30 g L-bed^{-1} and indicated that both film diffusion (3.2×10^{-3} cm s^{-1} to 22.6×10^{-3} cm s^{-1}) and surface diffusion (1.46×10^{-7} cm^2 s^{-1} to 5.64×10^{-7} cm^2 s^{-1}) resistances control the sorption process. It was shown that IX resins are an alternative for the removal of sulfate from mine waters; they ensure very low residual concentrations, particularly in effluents where the sulfate concentration is below the gypsum solubility threshold.

1. Introduction

Sulfide-bearing mine residues have been an import source of toxic metal and sulfate water and groundwater pollution, particularly in the form of acid (or neutral) mine drainages. This type of contamination is produced during the oxidation of sulfide minerals associated with either coal or nonferrous ores. Many mine sites have acid mine drainage or metal contaminated wastewaters, thus, the water quality needs to be regulated as the resulting effluent is toxic to the environment. While different processes have been proposed to remove toxic metals, the high sulfate content usually present in these drainages presents an environmental challenge.

Although not considered a high risk pollutant when compared to toxic metals and acids, sulfate in effluents and drainages are subject to regulations worldwide by environmental agencies because sulfate is related to concrete and steel corrosion as well as increased soil and water salinity. In drinking water, sulfate can affect taste and have laxative effects at concentrations in excess of 600 mg L^{-1} (Haghsheno et al., 2009). Therefore, the World Health Organization recommends that health authorities should be notified if sulfate concentrations in drinking water exceed 500 mg L^{-1}. Similarly, environmental agencies in mining countries limit sulfate in drainages or mining effluents to values between 250 mg L^{-1} and 500 mg L^{-1}. When a specific guideline for sulfate is not proposed, a limit for total dissolved solids is usually specified, implying that sulfate concentrations must comply with such limits (INAP, 2003).

Sulfate-containing wastewaters or mining drainages are usually treated by a combination of approaches including acid neutralization (when necessary), sulfate precipitation with lime (or limestone), reverse osmosis, electrodialysis, and adsorption. The

* Corresponding author. Tel.: +55 31 3559 1102; fax: +55 31 3559 1561.
E-mail addresses: damagui2000@yahoo.com.br (D. Guimarães), versiane@demet.em.ufop.br (V.A. Leão).

http://dx.doi.org/10.1016/j.jenvman.2014.06.006
0301-4797/

selection of these processes is determined by several factors such as chemical availability, local regulations, commercialization of the produced water, and process economics (INAP, 2003). Precipitation is usually the first choice in the treatment of mine waters; gypsum, ettringite, and barium sulfate precipitation are the main options (INAP, 2003). Barium sulfate precipitation ensures very low residual sulfate concentrations, however, barium compounds are usually expensive, and any Ba^{2+} ions remaining in solution are a much greater environmental concern. Ettringite precipitation can also effectively remove sulfate, although it requires an alkaline pH to function properly (Ferreira et al., 2012). The eMalahleni Project in South Africa, for instance, applies a sequence of oxidation and precipitation steps before pumping mining water to a membrane system that uses ultrafiltration and reverse osmosis to produce a <200 mg L^{-1} TDS water. This water is subsequently chlorinated and sold as potable water (Hutton et al., 2009). Sulfate removal by shrimp peelings (Moret and Rubio, 2003), modified zeolites (Oliveira, 2006), and coconut pith (Namasivayam and Sangeetha, 2008) has also been proposed.

An alternative to membrane technology is ion exchange (IX), which is also capable of producing drinking water from mine drainages. Several processes utilizing IX have already been proposed; the Sulf-IX (formerly GYP-CYX) process is one example (INAP, 2003). In a study performed by Feng et al. (2000), a process for AMD treatment comprising an initial metal precipitation step followed by sulfate sorption on IX resins was devised. In addition, Haghsheno et al. (2009) investigated equilibrium and kinetic parameters related to sulfate removal from industrial wastewaters in fixed bed columns utilizing the Lewatit K 6362 anion exchange resin. Despite such studies, a fundamental assessment of sulfate sorption mechanisms is yet to be conducted. This is because most papers have addressed sulfate sorption kinetics using empirical kinetic models instead of a mass transfer analysis, particularly in fixed-bed conditions. Because such an approach is important for predicting column behavior in large-scale operations, the present study sought to investigate equilibrium and fixed-bed sorption parameters related to sulfate sorption by strong base ion exchange resins.

2. Experimental

2.1. Resin and solutions

Purolite A500 is a strong base type 1 (quaternary ammonium) macroporous polystyrene resin with a 1.15 eq L^{-1} exchange capacity supplied in Cl^- form. For further resin details, the reader is referred to the Purolite website (Purolite, 2013). Prior to the experiments, the resin was dry sieved using Tyler sieves, and a particle size range of 0.71 mm–0.84 mm was selected for all experiments. Samples were kept under water for at least 40 h and used as such in all experiments, unless otherwise stated.

Sulfate solutions of different concentrations were prepared from analytical grade Na_2SO_4 (99% Synth). The solutions utilized for pH control were prepared from analytical grade HCl (37% Synth) or NaOH (99%, Synth). Calibration of pH meters was carried out with pH 4.0, 7.0, and 10.0 buffers (Synth).

2.2. Batch experiments

2.2.1. Effect of pH on sulfate loading

Batch experiments were performed by mixing 100 mL of sulfate solutions containing different concentrations (100 mg L^{-1}–1200 mg L^{-1}) of the anion with 1 mL of the swollen resin in 250-mL Erlenmeyer flasks. Each suspension was stirred at 200 min^{-1} in an orbital shaker (News Brunswick Innova 44) for 6 h at constant temperature (34 °C, 50 °C, and 70 °C). At the end of the experiment, the solution was filtered in a fast filter paper (J. Prolab), and the filtrate was analyzed for total sulfur by ICP–OES (Section 2.4). The pH was controlled (Digimed) at 2, 4, 6, 8, or 10 using either 1 mol/L HCl or 6 mol/L NaOH solutions. Sulfate loading in the resin was determined by mass balance.

2.2.2. Equilibrium experiments

The sorption equilibrium was investigated through sorption isotherms produced at different temperatures, which enabled a thermodynamic analysis of sulfate sorption. These experiments were conducted by mixing 1 mL of hydrated resin with 100 mL of sulfate solution containing 30–1800 mg L^{-1} sulfate in 250-mL Erlenmeyer flasks at pH 4.0. The resultant suspensions were stirred at 200 min^{-1} in an orbital shaker (News Brunswick Innova 44). The experiments ran for 6 h (defined from the kinetics experiments), and the pH was maintained at the desired value with NaOH and HCl solutions. Temperature was varied from 22 °C to 70 °C. At the end of the experiment, the solution was filtered and assayed for total sulfur by ICP–OES (Section 2.4). Sulfate loading in the resin was determined by mass balance. Experimental data was then fitted to the Langmuir model. Afterward, the Van't Hoff equation was applied to calculate the values of ΔH and ΔS.

2.2.3. Sorption kinetics

Kinetic studies were performed by mixing 300 mg L^{-1} sulfate solution with 5 mL of hydrated resin in a 2-L Erlenmeyer flask maintained under agitation (200 min^{-1}; Ika) at 28 ± 1 °C in a temperature-controlled room. Solution pH was kept at 4.0. Samples were withdrawn every 5 min in the first hour, every 10 min in the second hour, and every 30 min afterwards up to 360 min. After filtration, the samples were assayed for total sulfur by ICP–OES. Experimental data were then fit to the pseudo-first order and pseudo-second order kinetic models, and also to the intraparticle diffusion model (Qiu et al., 2009).

2.3. Fixed-bed experiments

Fixed-bed experiments were carried out in a temperature-controlled room at 28 ± 1 °C. Different volumes of resin (with particle size ranging from 0.71 to 0.84 mm) were loaded on an unjacketed glass column (13 mm diameter × 142 mm height) to produce bed lengths of 60 mm, 90 mm, and 120 mm. After loading, distilled water was passed through the column for 60 min to remove fine particles that could have been loaded in the column. The column was fed upwards by peristaltic pumps (Millan) to avoid any preferential solution pathways. The flow rate (Q) was varied between 10 mL min^{-1} and 20 mL min^{-1}. Samples were collected regularly from the column effluent, and the sulfate concentration in the samples was analyzed by ICP–OES (Section 2.4). The inlet sulfate concentration (C_0) ranged from 115 mg L^{-1} to 340 mg L^{-1} (at pH 4.0), and the anion loading on the resin was determined by mass balance. The breakthrough data were fitted to the model proposed by Miura and Hashimoto (1977) using the Mathematica 9.0 package.

2.4. Analysis

An ICP–OES (Spectro, model Cirus CCD) was utilized for total sulfur (S_{total}) analysis, which was assumed to represent the sulfate concentration because experimental solutions were produced from sodium sulfate, and thus no other sulfur species were expected in the system. These analyses were performed without further treatment after sample filtration by fast filter paper (7.50 μm porosity, J. Prolab) and dilution with MilliQ water. A calibration curve was

produced from a 1000 mg/L sulfate stock solution prepared from a 1000-mg sulfate tritisol ampoule (Merck, 109872) and MilliQ water.

3. Results and discussion

3.1. Batch experiments

3.1.1. Sorption kinetics

The kinetic parameters related to sulfate sorption by the strong base ion exchange resin Purolite A500 were determined batchwise using sodium sulfate solutions at pH 4.0 and a temperature of 28 ± 1 °C. This pH value was selected because it is characteristic of many acid mine drainages. Sorption kinetics may be controlled by several processes including (i) film diffusion, (ii) intraparticle (pore) diffusion, and (iii) ion exchange onto sorption sites. Sorption models developed from chemical reaction kinetics usually consider the whole sorption process without distinction regarding these three steps. As shown in Fig. 1(a), sulfate sorption by Purolite A500 is fast; after 20 min, there is no change in the sulfate loading on the resin, which reached a loading of 24.5 mg SO_4^{2-} mL-resin^{-1}.

The data presented in Fig. 1(a) were then fitted to the pseudo-first order, pseudo-second order, and intraparticle diffusion models. The pseudo-first-order model has been widely used to describe the sorption of pollutants from wastewater, but it can only be applied to model sorption kinetics at low resin loadings (far from equilibrium). Accordingly, as presented in Fig. 1(b), this model described the first 20 min of the sulfate sorption process. The resultant rate constant of 0.023 min^{-1} (r^2 = 0.933) suggested film diffusion as the controlling mechanism during batch sorption. The pseudo-second order model produced a worse fit to the same data (r^2 = 0.88), whereas the intraparticle model could not describe sulfate sorption by the strong base resin. The results of the current

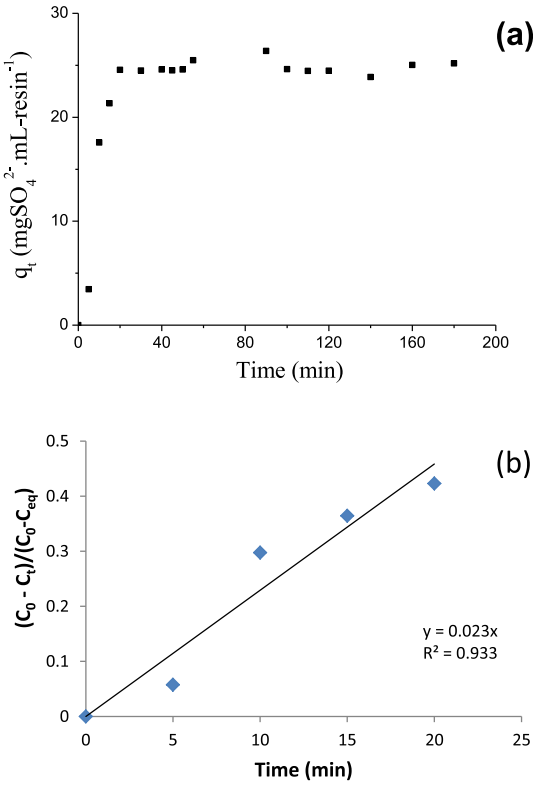

Fig. 1. Kinetics of sulfate sorption by Purolite A500 (a) and fitting to the pseudo-first order model (b). Experimental conditions: 1 mL-resin, 100 mL solution, 200 cm^{-1}, 28 °C.

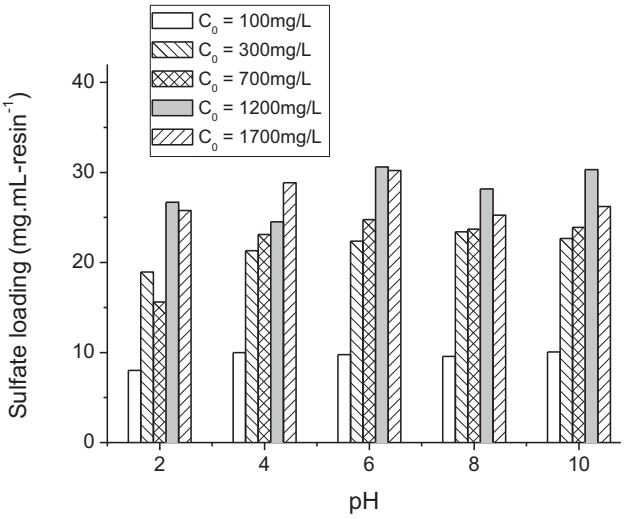

Fig. 2. Effect of pH on sulfate sorption on Purolite A500 strong base ion exchange resins at 34 °C different initial sulfate concentrations. Experimental conditions: 1 mL-resin, 100 mL solution, 200 cm^{-1}.

study are consistent with the work of Haghsheno et al. (2009), who applied the reversible first-order kinetic model to sulfate uptake by Lewatit K6362 (type 1 strong base resin); Haghsheno et al. (2009) found an overall rate constant of 0.062 min^{-1} for a 500 mg L^{-1} sulfate mine water.

3.1.2. Effect of pH on sulfate loading

The effect of pH on sulfate sorption was examined by mixing different sulfate concentrations (1001700 mg L^{-1}) with the ion exchange resin in batch conditions. Experiments were carried out at 34 °C, 50 °C, and 70 °C; only the 34 °C results are shown in Fig. 2 because the results observed at 50 °C and 70 °C followed a similar trend. As expected, sulfate sorption in Purolite A500 increased with the initial aqueous sulfate concentration. Sorption reached a maximum of approximately 30 mg mL-resin^{-1}, for the initial SO_4^{2-} concentrations of 1200 mg L^{-1} and 1700 mg L^{-1}. Larger resin loadings were likely limited by the nature of the batch experiment. The small effect of pH on sulfate uptake by Purolite A500 was derived from the strong base character of the resin, indicating that the exchange capacity was not affected by the solution pH. Values of pH above 10 were not tested because this is the highest pH at which effluents can be discharged according to most environmental regulations. However, it is believed that sulfate sorption would follow the same pattern observed at pH 8.0 and 10.0. Similar loadings were observed during sulfate uptake by modified coconut fibers by Lima et al. (2012), although the authors did not investigate the effect of pH on sulfate sorption by the bio-sorbent. During sulfate sorption on chitinous materials, very high sulfate loadings were measured (157 mg g-chitin^{-1}); however, the loading capacity significantly decreased at pH values above 6 due to the loss of protonated amine groups in the biomaterial network (Moret and Rubio, 2003).

3.1.3. Effect of temperature

Fig. 3(a) presents isotherms describing sulfate sorption by the Purolite A500 strong base resin at pH 4 and different temperatures (22 °C–70 °C). Resin loadings were fitted to the Langmuir equation, as shown in Fig. 3(a). The constant b on the Langmuir isotherm increased with temperature in the range of 22 °C–70 °C. Thus, it is suggested that sulfate sorption on Purolite A500 was both a favorable and nonideal reversible process, as expected. The values

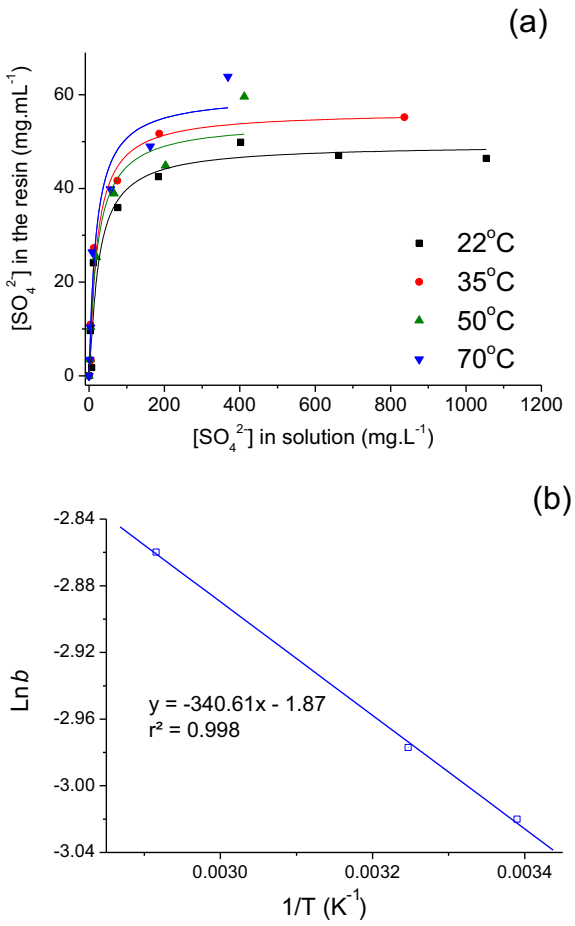

Fig. 3. Fitting sulfate sorption isotherm to initial sulfate concentrations according to the Langmuir equation (a). Application of the Vant Hoff equation to sulfate sorption (b). Experimental conditions: 1 mL-resin, 100 mL solution, 200 cm^{-1}; 34 °C (a) and 50 °C (b).

of q_{max} vared between 49.4 mg mL-resin^{-1} and 59.6 mg mL-resin^{-1} with increasing temperature (Table 1). These values were close to the reported exchange capacity of the resin (1.15 meq mL^{-1}) and higher than the values observed in modified coconut fibers (31.2 mg g^{-1}) (Lima et al., 2012), limestone (23.7 mg g^{-1}) (Silva et al., 2012b), and a mesoporous silica and cationic surfactant composite material (3.86 mg g^{-1}) (Clark and Keller, 2012).

The effect of temperature on sulfate sorption was analyzed by applying the Van't Hoff equation to the equilibrium constant b (Langmuir equation) at different temperatures, as depicted in Equation (1) (Karthikeyan et al., 2005; Wu et al., 2009). Both enthalpy and entropy of sorption were estimated from b values at different temperatures.

$$\mathrm{Ln}b = -\frac{\Delta H}{RT} + \frac{\Delta S}{R} \quad (1)$$

Applying Equation (1) to the experimental data (Fig. 3(b)), the sorption enthalpy was determined to be +2.83 kJ mol^{-1}, implying that sulfate sorption on Purolite A500 was an endothermic physisorption process (Lv et al., 2008). This effect may be related to a stronger swelling of the resin and a faster diffusion of sulfate ions at higher temperatures (Al Hamouz and Ali, 2012). The contribution to entropy from sulfate sorption (−15.5 J mol^{-1} K^{-1}) suggested a decrease in randomness at the resin-solution interface, as also observed by Torab-Mostaedi et al. (2010) in a study addressing toxic metal sorption in perlite. Moreover, the negative values of free energy confirmed the spontaneous nature of the sorption process.

3.2. Fixed-bed sorption

Sulfate removal from aqueous solutions in fixed-bed experiments was also investigated. Specifically, the effects of bed height (Z), flow rate (Q), and initial sulfate concentration (C_0) on sulfate sorption by Purolite A500 ion exchange resin were studied at pH 4.0 and 28 ± 1 °C. Table 2 depicts the key experimental parameters related to the breakthrough curves presented in Fig. 4. The breakthrough point was selected as 0.05 of C_0, while the saturation point was taken as 0.95 of C_0.

As expected, breakthrough time (t_b) was reduced at higher inlet sulfate concentrations and shorter bed depths. This result can be explained by the fact that the total number of sulfate sorption sites in the experiments was finite; thus, either an increase in C_0 or a decrease in bed depth resulted in a faster exhaustion of sorption sites. Moreover, the driving force of sorption was reduced with increasing surface coverage, hampering sulfate uptake. Decreasing the flow rate increased t_b, and therefore, V_b (the volume of solution treated at the breakthrough) because the sorption zone took longer to reach the top of the column, facilitating mass transfer (Srivastava et al., 2008). Modifying the flow rate did not seem to affect the shape of the breakthrough curve, and the classical S-shape was observed regardless of the flow rate, as will be discussed next.

Fixed-bed sulfate sorption was modeled by applying the model of Miura and Hashimoto (1977). This model was developed under two approximations: the constant pattern of concentration distribution and linear driving force (LDF). Different solutions were proposed for the Freundlich and Langmuir isotherms, and those related to the latter are presented in Equation 2 through 11.

$$\xi = \frac{kf.au}{ks.au}.\frac{C_0}{q_{max}} \quad (2)$$

$$ks.au = \frac{60.Ds.\rho_B}{dp^2} \quad (3)$$

$$au = \frac{6}{dp}(1-\varepsilon) \quad (4)$$

$$\theta_t = \frac{ks.au}{\rho_B\left(1+\frac{1}{\xi}\right)}.\left(t - \frac{\varepsilon_B Z}{U}\right) \quad (5)$$

$$X_t = \frac{ks.au}{1+\frac{1}{\xi}}.\frac{q_{max}}{C_0}\frac{Z}{U} \quad (6)$$

$$\varphi_1 = \frac{1}{1-La}\ln[X_{int}] - \frac{La}{1-La}\ln[1-X_{int}] - \ln[(La+(1-La)X_{int})] - \frac{La}{1-La}\ln[La] + 1 \quad (7)$$

Table 1
Langmuir model parameters for sulfate sorption on A500 resin at different temperatures.

Temperature (°C)	r^2	b (L mg^{-1})	Q_{max} (mg mL-resin^{-1})
22	0.940	0.04880	49.406
34	0.965	0.05094	56.436
50	0.968	0.04603	54.319
70	0.956	0.05728	59.568

Table 2
Breakthrough parameters for sulfate sorption on Purolite A500 in fixed-bed experiments, at 28 ± 1 °C.

Z (cm)	Q ($cm^3\ min^{-1}$)	C_0 ($g\ L^{-1}$)	U ($cm\ min^{-1}$)	t_b (min)	V_b (mL)	t_e (min)	V_e (mL)	ε_B
9	15	0.115	11.3	190	2850	230	3450	0.35
9	15	0.17	11.3	80	600	190	3300	0.35
9	15	0.35	11.3	20	300	100	1500	0.35
6	15	0.17	11.3	40	600	150	2250	0.33
9	15	0.17	11.3	80	1200	190	2850	0.35
12	15	0.17	11.3	110	1650	230	3450	0.31
9	10	0.17	7.5	150	1500	260	2600	0.35
9	15	0.17	11.3	80	600	190	2400	0.35
9	20	0.17	15.1	50	1000	140	2800	0.35

$$\varphi_2 = \frac{\mathrm{La}}{1-\mathrm{La}}\ln X_{\mathrm{int}} - \frac{\mathrm{La}}{1-\mathrm{La}}\ln[1-X_{\mathrm{int}}] - 1 \tag{8}$$

$$\eta = 1 - 0.192^{*}(1-\mathrm{La})^3 \tag{9}$$

$$\theta_t - X_t = \frac{1}{1+\xi}\varphi_1 + \frac{\xi}{1+\xi}\frac{1}{\eta}\varphi_2 \tag{10}$$

Bulk (X) and interface (X_{int}) concentrations are related through Equation (11).

$$X = \frac{(\xi\mathrm{La}+\eta)X_{\mathrm{int}} + \xi(1-\mathrm{La})X_{\mathrm{int}}^2}{(\xi+\eta)[\mathrm{La}+(1-\mathrm{La})X_{\mathrm{int}}]} \tag{11}$$

This model assumes that the resistances associated with fluid-film and solid phase diffusion are important for the process, and thus the adsorbate bulk concentration is different from that at the interface (due to the fluid film resistance). This model was selected because it can be easily applied to the experimental data, and more importantly because a previous work on Cl^- to SO_4^{2-} exchange on quaternary-ammonium resins confirmed diffusion as the rate-controlling step (Liberti et al., 1987). The system of Equations (2)–(11) was solved using the Mathematica 9.0 package, producing the film (kf) and surface diffusion (Ds) coefficients depicted in Table 3. Model fitting to the experimental data is depicted in Fig. 4, which indicates that the Miura and Hashimoto model (1977) successfully described the breakthrough curves developed during sulfate sorption on Purolite A500 resin. The agreement between the experimental data and those predicted by the model is reflected by the low values of the SSE parameter seen in Table 3.

Flow rate was expected to affect film diffusion because higher flow rates decrease film resistance, which would produce larger kf values. Indeed, Table 3 shows an increase in the film diffusion coefficient (from 4.56×10^{-3} cm s^{-1} to 6.66×10^{-3} cm s^{-1}) as the flow rate increased from 10 mL min^{-1} to 20 mL min^{-1}. Conversely, as the sulfate concentration increased from 115 mg L^{-1} to 350 mg L^{-1}, this coefficient decreased from 22.59×10^{-3} cm s^{-1} to 3.37×10^{-3} cm s^{-1}. A similar effect was observed during phenol sorption on fly ash (Srivastava et al., 2008). Fig. 4(a) shows that the beginning of the breakthrough curve was sharper as compared to the other two investigated concentrations. This can be ascribed to the slower saturation of the resin sites, which resulted in the better utilization of the loading capacity of the resin. Although the film diffusion coefficient was not expected theoretically to vary with bed depth, it was herein observed that increasing bed depth slightly decreased the film diffusion coefficient, as observed in many other studies (Patel and Vashi, 2012; Silva et al., 2012a; Srivastava et al., 2008). This effect might be related to an increased resistance to fluid flow at higher bed depths. However, such behavior requires further investigation.

According to the literature, the strongest effect on the shape of the breakthrough curve is produced by surface diffusivity (Ds), particularly in the region of the saturation point whenever

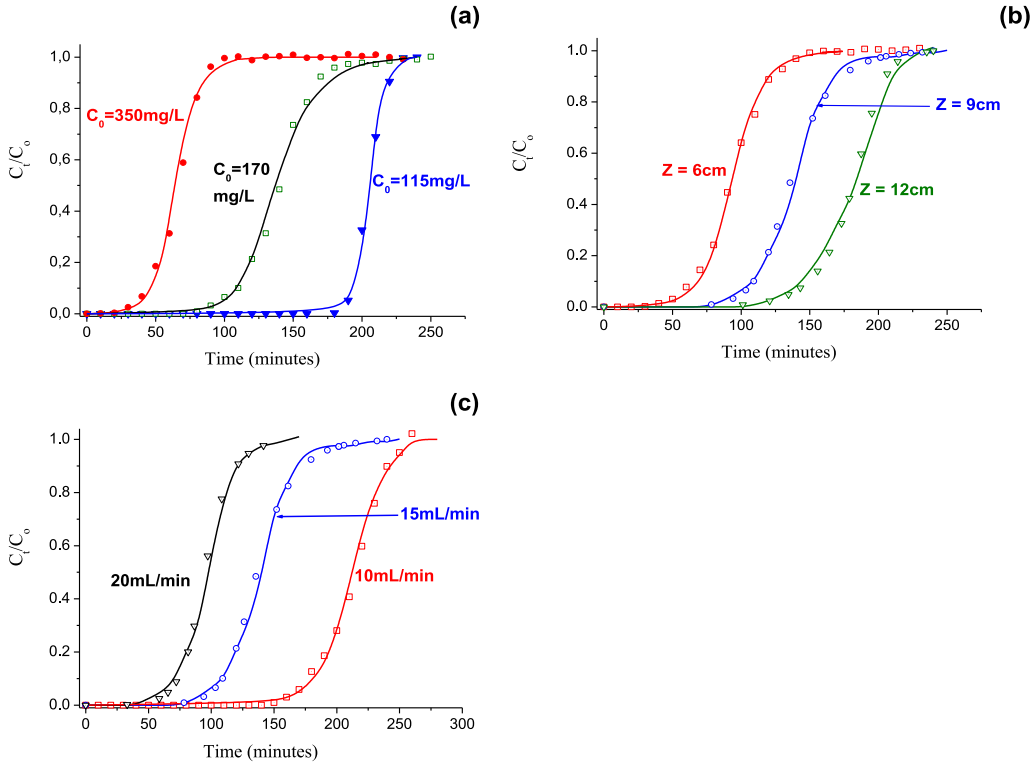

Fig. 4. Effect of different parameters on the sulfate sorption on Purolite A500 strong base ion exchange resins. Different initial concentrations at $Q = 15$ mL min^{-1} and H = 9 cm (a); column depth, at $C_0 = 170$ mg.L^{-1} and $Q = 15$ mL min^{-1} (b); flow rate, at $C_0 = 170$ mg.L^{-1} and H = 9 cm (c).

Table 3
Parameters predicted according to the Miura and Hashimoto model (1977) for sulfate sorption on Purolite, at 28 ± 1 °C.

Z (cm)	Q (cm^3 min^{-1})	C_0 (g L^{-1})	ρB	k_f (cm^2 s^{-1})	Ds (cm^2 s^{-1})	q (g L-resin^{-1})	N (g L-bed^{-1})	SSE	ξ
9	15	0.115	0.68	2.26E-02	5.64E-07	36.70	23.86	43.0	0.787
9	15	0.17	0.60	4.92E-03	1.46E-07	40.40	26.26	1711.2	1.135
9	15	0.35	0.64	3.37E-03	2.27E-07	50.10	32.57	586.0	0.929
6	15	0.17	0.68	5.87E-03	1.69E-07	51.70	33.61	1069.2	1.024
9	15	0.17	0.60	4.92E-03	1.46E-07	40.40	26.26	1711.2	1.135
12	15	0.17	0.66	3.19E-03	2.88E-07	46.60	30.29	273.5	0.354
9	10	0.17	0.69	4.56E-03	1.60E-07	43.00	27.95	122.4	0.816
9	15	0.17	0.60	4.92E-03	1.46E-07	40.40	26.26	1711.2	1.135
9	20	0.17	0.63	6.66E-03	1.62E-07	46.60	30.29	189.8	1.351

intraparticle diffusion is the rate-limiting transport process. Conversely, the effect of the external mass transfer coefficient is noticed mainly in the vicinity of the breakthrough point. No trend in Ds values was observed in Table 3. This suggests that the effective diffusion coefficient was not a function of sulfate concentration, which is in contrast to the results of other studies (Serarols et al., 1999). Surface diffusivity did not vary with solution flow rate because the latter does not have any effect on diffusion inside the resin pores (Helferrich, 1962). Regardless of the parameter investigated, the calculated Ds values were of the same order of magnitude (1.46 cm^2 s^{-1} to 5.64 × 10^{-7} cm^2 s^{-1}) and were quite similar to the value of 8 × 10^{-7} cm^2 s^{-1} reported for sulfate sorption on the strong base gel resin Amberlite IRA 400 (Liberti et al., 1978).

The parameter ξ, as proposed by Miura and Hashimoto (1977) and classically represented as the Biot number (Sperlich et al., 2008), expresses the effects on the sorption process by resistances related to mass transport in the boundary layer and diffusion in the resin pores.

Values of ξ much higher than one ($\xi \to \infty$) indicate that diffusion in the particle pores is the controlling step, whereas ξ values much lower than 1 ($\xi \to 0$) indicate film diffusion control. As shown in Table 3, ξ values around 1 suggested that the resistances related to both film and surface diffusion were similar in magnitude in the current study. As stated, few works have addressed sulfate sorption by ion exchange resins, and a direct comparison with the literature was difficult.

4. Conclusions

Sulfate removal remains a challenge in the management of acid mine drainage. The universally applied treatment in which AMD is mixed with lime to precipitate gypsum results in at least 1200 mg L^{-1} sulfate in the final effluent. As this concentration needs to be further reduced to values below to the 250 mg L^{-1} – 400 mg L^{-1} range, other techniques must be also applied. The current work showed that strong base type 1 IX resins can reduce sulfate values, thus enabling compliance with most environmental regulations. Sulfate sorption on Purolite 1500 was a pH-independent and endothermic process (+2.83 kJ mol^{-1}) that could be represented at equilibrium by the Langmuir isotherm with maximum loadings (Qmax) of up to 60 mg SO_4^{-2} mL-resin^{-1}. A deeper understanding of the mechanisms related to fixed-bed sulfate removal by such materials was also provided, indicating that both film and surface diffusion controlled the rate of sulfate sorption by the Purolite A500 resin. Surface diffusivities (Ds) were similar to those reported for sulfate sorption on other strong base resins.

Acknowledgments

Financial support from the funding agencies FINEP, FAPEMIG, CNPq, CAPES, and Vale is gratefully appreciated.

Nomenclature

au	specific surface area in the bed
b	Langmuir constant (L mg^{-1})
C_0	initial solute concentration (mg L^{-1})
C_{eq}	equilibrium solute concentration (mg L^{-1})
C_t	solute concentration at time t (mg L^{-1})
dp	particle diameter
Ds	surface diffusivity (cm^2 s^{-1})
k_f	film diffusion coefficient (cm^2 s^{-1})
m	mass of sorbent in the column (g)
La	separation factor for the Langmuir isotherm
N	sorptive capacity of the bed (g L-bed^{-1})
Q	flow rate (mL min^{-1})
q_e	equilibrium sorption capacity (mg g^{-1})
q_{max}	maximum loading according to the Langmuir equation (mg g^{-1})
q_t	sorption capacity (mg g^{-1}) at time t
SSE	sum of squared errors
t	time (min)
t_b	breakthrough time (min)
t_e	exhaustion time (min)
U	linear flow velocity of the feed to the bed (mL min^{-1})
U_t	fractional attainment of equilibrium
V_b	volume of solution treated at the breakthrough point (dm^3)
Ve	exhaustion volume (mL)
X	bulk dimensionless concentration
X_{int}	interface dimensionless concentration
X_t	dimensionless column length (Equation (6))
Z	bed height (cm)
ΔH	enthalpy
ΔS	entropy

Greek letters

ρ_p	particle density
ρ_B	bed density
ε_B	bed porosity
ξ	(kf.au/ks.au).C_0/q_{max}
η	correction factor for ks.au
θ_t	dimensionless time

References

Al Hamouz, O.C.S., Ali, S.A., 2012. Removal of heavy metal ions using a novel cross-linked polyzwitterionic phosphonate. Sep. Purif. Technol. 98, 94–101.
Clark, K.K., Keller, A.A., 2012. Adsorption of perchlorate and other oxyanions onto magnetic permanently confined micelle arrays (Mag-PCMAs). Water Res. 46, 635–644.
Feng, D., Aldrich, C., Tan, H., 2000. Treatment of acid mine water by use of heavy metal precipitation and ion exchange. Min. Eng. 13, 623–642.
Ferreira, B.C.S., Lima, R.M.F., Leão, V.A., 2012. Remoção de sulfato de efluentes industriais por precipitação. Eng. Sanit. Ambient. 16, 1–8.

Haghsheno, R., Mohebbi, A., Hashemipour, H., Sarrafi, A., 2009. Study of kinetic and fixed bed operation of removal of sulfate anions from an industrial wastewater by an anion exchange resin. J. Hazard. Mater. 116, 961–966.
Helferrich, F., 1962. Ion Exchange. McGraw-Hill, New York.
Hutton, B., Kahan, I., Naidu, T., Gunther, P., 2009. Operating and maintenance experience at the Emalahleni water reclamation plant. In: International Mine Water Conference, pp. 415–430. Pretoria, South Africa.
INAP, 2003. Treatment of Sulphate in Mine Effluents. International Network for Acid Prevention, p. 129.
Karthikeyan, T., Rajgopal, S., Miranda, L.R., 2005. Chromium(VI) adsorption from aqueous solution by Hevea Brasilinesis sawdust activated carbon. J. Hazard. Mater. 124, 192–199.
Liberti, L., Boari, G., Passino, R., 1978. Chloride/sulfate exchange on anion resins. Kinetic investigations II. Particle diffusion rates. Desalination 25, 123–134.
Liberti, L., Petruzzelli, D., Helfferich, F.G., Passino, R., 1987. Chloride/sulfate ion exchange kinetics at high solution concentration. React. Polym. Ion Exch. Adsorb. 5, 37–47.
Lima, A.C.A., Nascimento, R.F., Sousa, F.F., Filho, J.M., Oliveira, A.C., 2012. Modified coconut shell fibers: a green and economical sorbent for the removal of anions from aqueous solutions. Chem. Eng. J. 185–186, 274–284.
Lv, L., Wang, Y., Wei, M., Cheng, J., 2008. Bromide ion removal from contaminated water by calcined and uncalcined MgAl-CO_3 layered double hydroxides. J. Hazard. Mater. 152, 1130–1137.
Miura, K., Hashimoto, K., 1977. Analytical solutions for the breakthrough curves of fixed-bed adsorbers under constant pattern and linear driving force approximations. J. Chem. Eng. Jpn. 10, 490–493.
Moret, A., Rubio, J., 2003. Sulphate and molybdate ions uptake by chitin-based shrimp shells. Min. Eng. 16, 715–722.
Namasivayam, C., Sangeetha, D., 2008. Application of coconut coir pith for the removal of sulfate and other anions from water. Desalination 219, 1–13.
Oliveira, C.R., 2006. Adsorção – remoção de sulfato e isopropilxantato em zeólita natural funcionalizada, Mining Engineering. Universidade Federal do Rio Grande do Sul, Porto Alegre, p. 107.
Patel, H., Vashi, R.T., 2012. Fixed bed column adsorption of ACID yellow 17 dye onto tamarind seed powder. Can. J. Chem. Eng. 90, 180–185.
Purolite, 2013. Purolite® A500/2788-Macroporous type 1 Strong Base Anion Exchange Resin.
Qiu, H., Lv, L., Pan, B.C., Zhang, Q.J., Zhang, W.M., Zhang, Q.X., 2009. Critical review in adsorption kinetic models. J. Zhejiang Univ. Sci. A 10, 716–724.
Serarols, J., Poch, J., Llop, M.F., Villaescusa, I., 1999. Determination of the effective diffusion coefficient for gold(III) on a macroporous resin XAD-2 impregnated with triisobutyl phosphine sulfide. React. Funct. Polym. 41, 27–35.
Silva, A.M., Cordeiro, F.C.M., Cunha, E.C., Leão, V.A., 2012a. Fixed-bed and stirred-tank studies of manganese sorption by calcite limestone. Ind. Eng. Chem. Res. 51, 12421–12429.
Silva, A.M., Lima, R.M.F., Leão, V.A., 2012b. Mine water treatment with limestone for sulfate removal. J. Hazard. Mater. 221–222, 45–55.
Sperlich, A., Schimmelpfennig, S., Baumgarten, B., Genz, A., Amy, G., Worch, E., Jekel, M., 2008. Predicting anion breakthrough in granular ferric hydroxide (GFH) adsorption filters. Water Res. 42, 2073–2082.
Srivastava, V.C., Prasad, B., Mishra, I.M., Mall, I.D., Swamy, M.M., 2008. Prediction of breakthrough curves for sorptive removal of phenol by Bagasse fly ash packed bed. Ind. Eng. Chem. Res. 47, 1603–1613.
Torab-Mostaedi, M., Ghassabzadeh, H., Ghannadi-Maragheh, M., Ahmadi, S.J., Taheri, H., 2010. Removal of cadmium and nickel from aqueous solution using expanded perlite. Braz. J. Chem. Eng. 27, 299–308.
Wu, Y., Li, B., Feng, S., Mi, X., Jiang, J., 2009. Adsorption of Cr(VI) and As(III) on coaly activated carbon in single and binary systems. Desalination 249, 1067–1073.